Metallurgy and materials
*Metalurgia e materiais*

# Comparative assessment of microstructure and texture in the Fe-30.5Mn-8.0Al-1.2C and Fe-30.5Mn-2.1Al-1.2C steels under cold rolling

http://dx.doi.org/10.1590/0370-44672017700005

**Fabrício Mendes Souza**
Professor PhD
Universidade do Estado de Minas Gerais - UEMG
Divinópolis – Minas Gerais - Brasil
souzafm@yahoo.com.br

## Abstract

Investigation of microstructure and texture has been done for cold rolled Fe-30.5Mn-8.0Al-1.2C (8Al) and Fe-30.5Mn-2.1Al-1.2C (2Al) (wt.%) steels. They were rolled to a strain of ~0.70. Refinement of a crystallographic slip band substructure in low to medium rolling strain and nucleation of twins on the mature slip bands at a higher strain were suggested as deformation mechanisms in the 8Al steel. Mainly shear banding contributed to the formation of a Copper texture in such steel. Brass-texture development in the 2Al steel is mainly due to deformation twinning and shear banding formation. Detailed images of KAM maps showed that the stored deformation energy was mainly localized in the twinned areas and shear bands, which generated the inhomogeneous deformation microstructures in both steels at a higher strain. Goss and Brass texture intensity decreases and Cu-texture intensity increases as the Al wt.% increases in different cold rolled High-Mn (Mn ~30 wt.%) steels.

**Keywords:** austenitic steels; microstructures; crystallographic texture; deformation mechanisms, electron backscattering diffraction (EBSD); electron channeling contrast imaging (ECCI).

## 1. Introduction

Good combinations of strength, ductility (ultimate tensile strength UTS of 1.0-1.5 GPa and elongation of 30-80%) have been achieved by deforming austenitic high manganese lightweight steels. They are very attractive for structural applications and have a Mn content between 20 and 30 wt.%, Al additions ranged between 1 wt.% and 10 wt.%, and C between 0.5 and 1.8 wt.%. Activation of refined dislocation substructure and deformation twins provides the strain-hardening of the Fe-30.5Mn-2.1Al-1.2C (wt.%) (2Al) steel, which has a stacking fault energy (SFE) of 63 mJ $m^{-2}$. The SFE of the Fe-30.5Mn-8.0Al-1.2C (wt.%) (8Al) steel is 85 mJ $m^{-2}$. The methods used for calculation of their stacking fault energies can be found elsewhere (Gutierrez-Urrutia and Raabe, 2012, 2014). Recently Welsch *et al.* (2016) reported that very thin slip bands are formed by strong slip planarity, conducing a refined slip band structure during straining of such steel. It belongs to the group of dislocation-mediated plasticity steels and its deformation mechanism is known as dynamic slip band refinement.

TWIP steels have been extensively studied owing to their dependence on mechanical properties and deformation mechanisms. Microstructure development and crystallographic texture evolution upon deformation have been also considered (Bouaziz *et al.*, 2011 and De Cooman *et al.*, 2011). Alloy-type texture was observed for the 2Al steel and TWIP steels and pure metal-type for the 8Al steel with good similarity with other alloys. Slip and mechanical twinning activates the alloy-type texture. It has been associated to the brass texture after cold rolling. Furthermore, shear banding mainly contributes to the formation of Goss and Copper textures (Ray, 1995, Vercammen *et al.*, 2004, Bracke *et al.*, 2012, and Haase *et al.*, 2013).

In previous works, the aspects of texture and microstructure were separately examined for these 2Al and 8Al steels cold-rolled down to a strain of ~0.7 (Souza *et al*, 2016). In this work, it is suggested that dynamic slip band refinement may be the deformation mode at a low to medium strain level (~0.22), while at a higher strain level, the nucleation of twins may occur by the interaction of dislocation sources with the twinning partials on the mature slip bands for the 8Al steel based on a recently published work (Welsch *et al.*, 2016). Kikuchi pattern image quality (IQ) and Kernel average misoriantation (KAM) maps have been used here with detailed evaluation of the deformation heterogeneities (slip, shear band, and twinning) in regard to accommodation of deformation energy. They have been compared with the texture evolution for such steel. These finds have been also compared to those of the cold-rolled 2Al steel and other studied in TWIP steels. The importance of Al con-

tent increase on the texture of the alloys has been also evaluated from a general point of view. Electron backscatter diffraction (EBSD) and electron channeling contrast imaging (ECCI) were used to this characterization.

## 2. Experimental

The chemical compositions of the studied steels are Fe-30.5Mn-8.0Al-1.2C and Fe-30.5Mn-2.1Al-1.2C (wt. %). These steels were melted in an induction furnace under Ar atmosphere, and casted as 25 mm diameter ingot bars. The ingots were reheated to 1200°C during 30 minutes, hot-rolled down to 75% thickness reduction at 1100°C, and subsequently water quenched. These hot-rolled alloys were solution treated for two hours at 1100 °C under Ar atmosphere, and water quenched. The steels were also cold rolled down to thickness reductions between 10 and 50% with a thickness reduction step of 10%, as presented in Table I. The experiments were performed at the *Max-Planck-Institut für Eisenforschung GmbH* (MPIE) research institute.

| $e = (t0-t)/t0$ | 0.10 | 0.20 | 0.30 | 0.40 | 0.50 |
|---|---|---|---|---|---|
| $\varepsilon = \ln(t0/t)$ | 0.11 | 0.22 | 0.36 | 0.51 | 0.69 |

Table I
Engineering strain (e), and logarithmic true strain (ε) values of the cold-rolled 8Al and 2Al steels.

Details on the EBSD, ECCI, and results of IQ and KAM maps can be found in (Souza *et al.*, 2016). Herein the deformation energy accommodation on slip, shear band, and twinning has been characterized and differentiated on the deformed microstructure of the 8Al steel and compared to that of the 2Al steel. The ECCI technique was used to obtain micrographs of the deformed microstructure for the 8Al steel, at strains of 0.22 and 0.69, and to compare with the recently published ECCI micrographs of the same tensile tested steel studied in another work (Welsch *et al.*, 2016). Macrotexture results (copper, Goss, brass, S, and copper-twin texture components) were obtained from the inverse pole figures (IPF) of a previous work (Souza *et al.*, 2016).

## 3. Results

The 8Al steel has a grain size of 148 µm and 2Al steel of 102 µm. Grains deformed along the rolling direction were observed for both cold rolled steels. A river-like structure and a greenish blue color on the IPF map (Goss and brass texture, as observed by means of orientation distribution function, ODF, results) were found in the 2Al steel at a higher strain level. There was also revealed fish bone-like structure patterns and an eminent violet color on the IPF map (strong Copper texture occurrence, as also observed by means of ODF results) in the 8Al steel at this strain level (Souza *et al.*, 2016).

The relevant microstructural characteristics of the 2Al and 8Al steels at cold rolling degrees of 10%, 40%, and 50% reduction are illustrated by high resolution IQ maps in Fig. 1a and 1b. Only slip was activated at a low strain level of 0.11 (see also Fig. 5) and mechanical twinning and shear banding (SB) were observed for both steels at a high strain level (Souza et al., 2016). Red lines on the IQ maps are twin boundaries, and black lines are high angle grain boundaries. Fig 1c shows the respec-

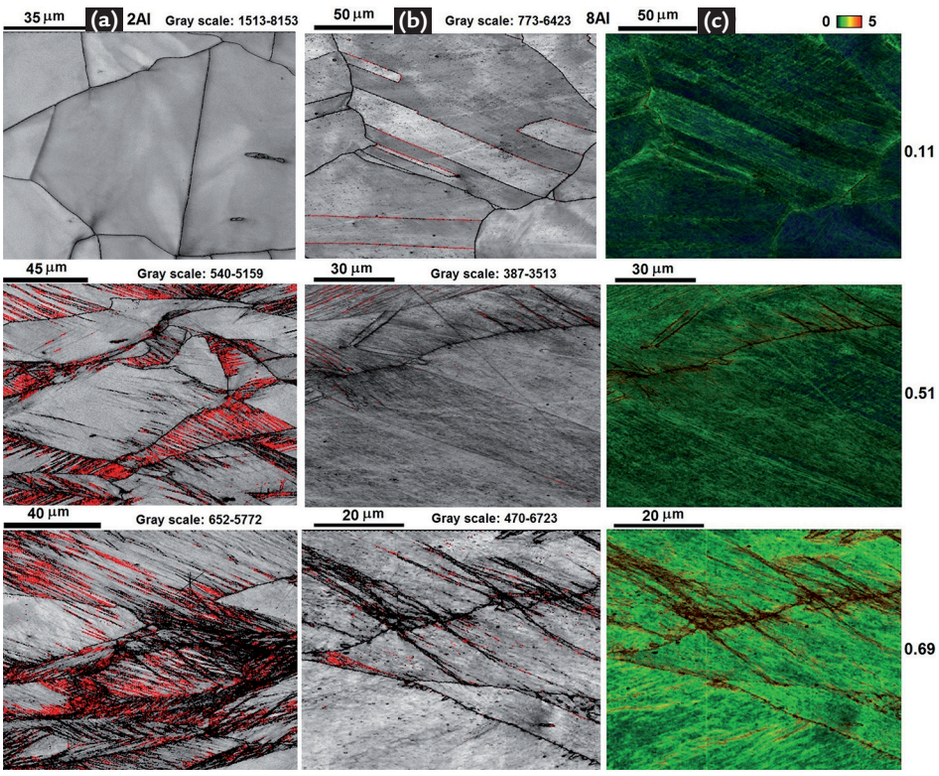


Figure 1
IQ maps of (a) 2Al steel and (b) 8Al at strain of 0.11, 0.51 and 0.69 showing their deformed microstructures. (c) KAM maps with angle range from 0° to 5° of the same strains for the 8Al steel. RD is the same shown in Fig. 2.

tive KAM maps from the microstructures of the 8Al steel at the same strain levels. Low variation in the KAM angle range is observed owing to deformation by slip at low strain level, while high variation in the KAM angle range can be seen for such steel at the higher strain level. Profuse mechanical twinning and SB at high strain level, and slip at low strain level evidenced that the deformation energy is accommodated with this same behavior in the 2Al steel (see Fig. 5).

Fig. 2 shows the ECCI micrographs showing the deformation mechanisms with more detailed aspects in the deformed microstructure of the 8Al steel at strains of 0.22 and 0.69. A similarity of the refined slip band microstructure related to the newly proposed deformation mechanism known as dynamic slip band refinement (Welsch *et al.*, 2016) may be observed in Fig. 2 at a strain of 0.22. SB with twins, crystallographic mechanical twinning, and remaining crystallographic slip band substructure can be observed in Fig. 2 at strain of 0.69. X like marks in Fig. 2 are {111} plane traces (Souza *et al.*, 2016).

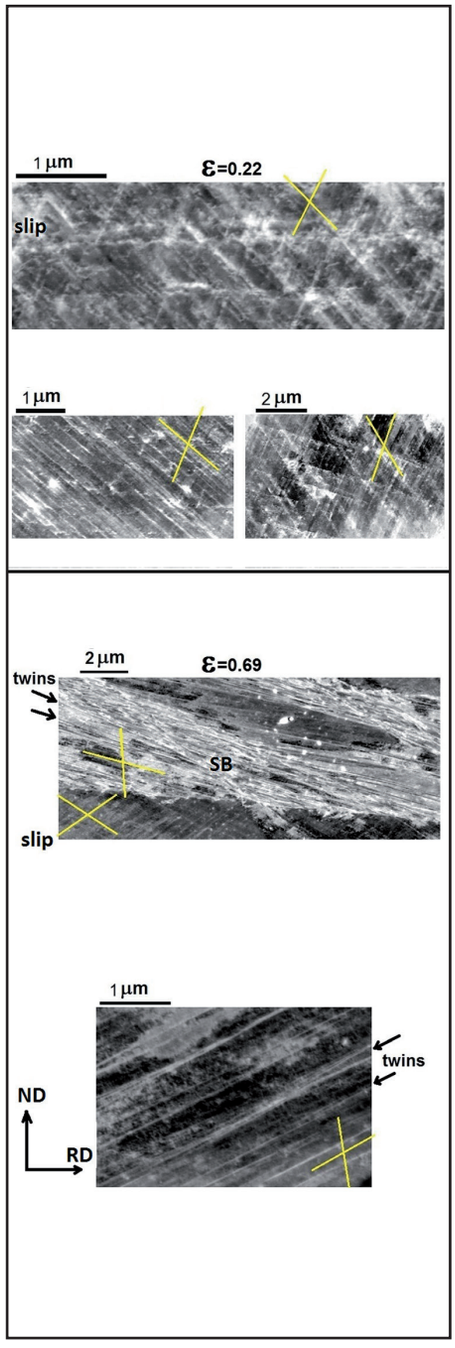


Figure 2
ECCI images showing slip band substructures and mechanical twins in the 8Al steel at strains of 0.22 and 0.69. X-like marks indicate the {111} slip planes. RD: rolling direction, ND: normal direction.

Intensities of the main texture components (copper Cu, Goss G, brass B, S, and copper-twin, CuT) and orientation distribution functions (ODFs), on the $\varphi_2$=45, $\varphi_2$=65, and $\varphi_2$=90 sections, with increasing cold rolling strain are shown in Fig. 3 for both steels. Fig. 3 also shows the graphs of the number fraction of the misorientation angle distributions obtained from EBSD macrotexture results, where the misorientation angle of 60° indicates that activation of twinning in the 2Al steel is easier than that in the 8Al steel, at a strain of 0.69. Strong B- and G-texture with CuT occurrence can be seen for the 2Al as observed in other high-Mn TWIP steels (Vercammen *et al.*, 2004, Bracke *et al.*, 2012, and Haase *et al.*, 2013). Cu-texture and occurrence of the G, B, and S texture components can be also observed for the 8Al, at a higher strain. More detailed texture aspects for these materials can be found in (Souza *et al.*, 2016).

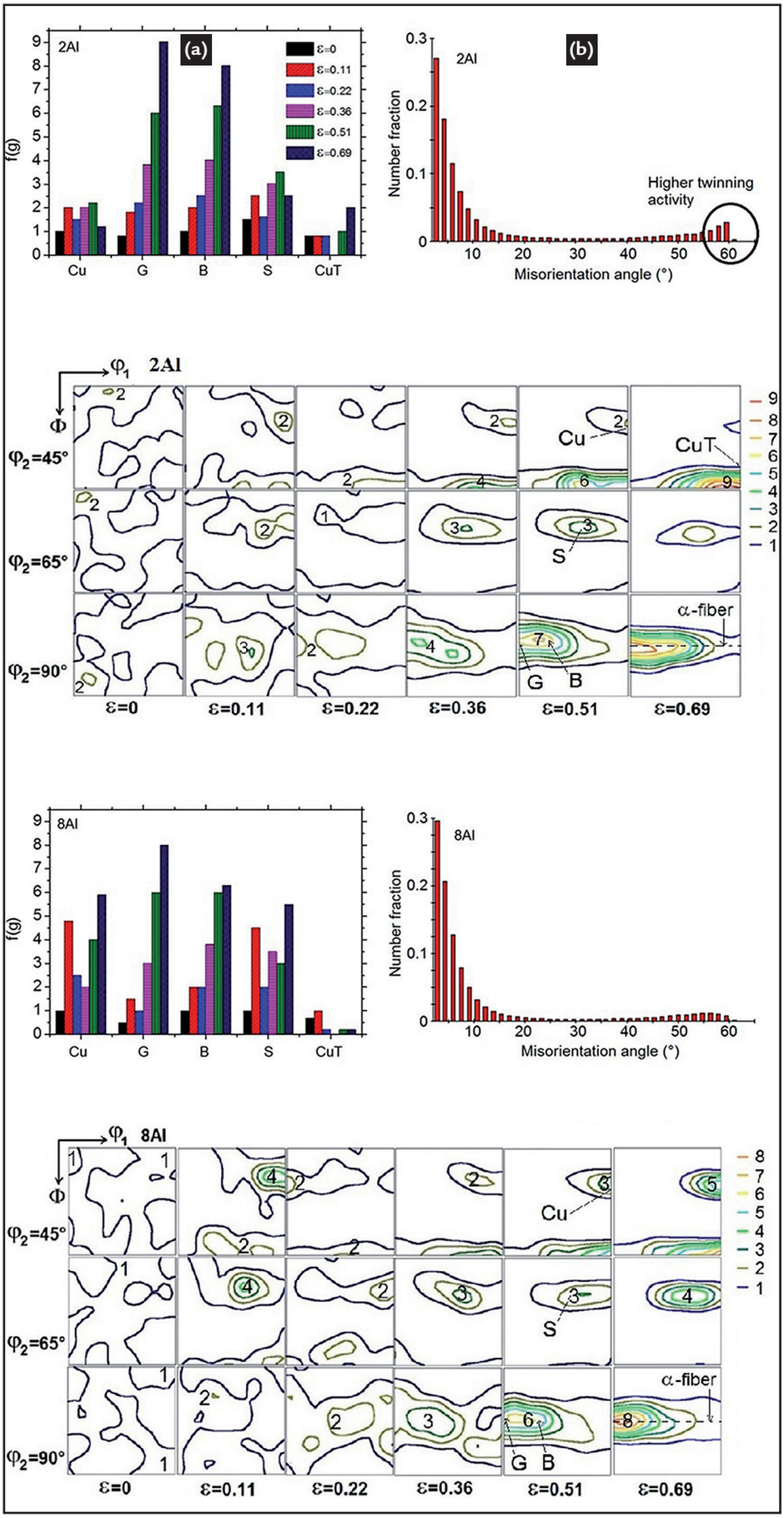


Figure 3
(a) Maximum intensities of the main orientations and orientation distribution functions (ODFs), on the $\varphi_2$=45, $\varphi_2$=65, and $\varphi_2$=90 sections, with increasing strain, and (b) number fractions of the misorientation angle distributions obtained from macrotexture results at strain of 0.69 for the 2Al and 8Al steels.

In Fig. 4 the intensities on the brass, Goss, and copper components as a function of Al content can be seen for different cold rolled high-Mn steels at strain of 0.69. It is relevant to observe the diminution of brass- and Goss-type texture intensities, whereas Copper-type texture intensity increases with increasing Al content.

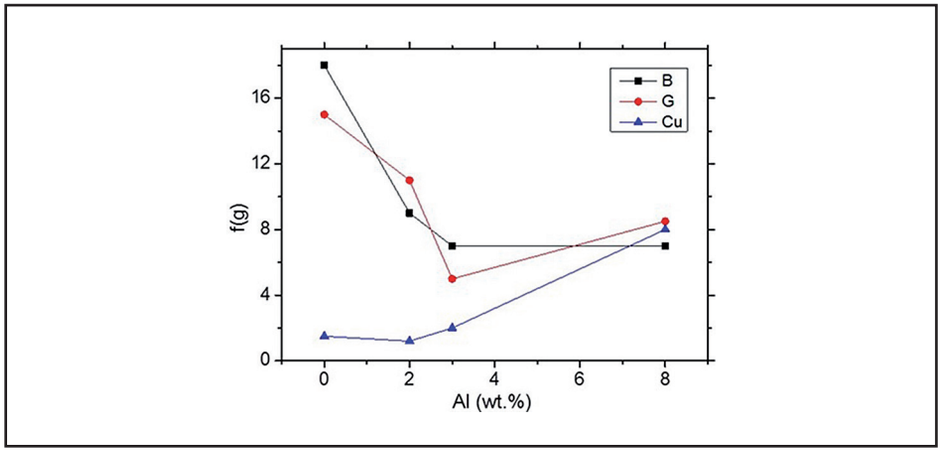


Figure 4
Intensities of the B, G, and Cu texture components with increasing Al content for the cold rolled Fe-28Mn-0.28C (Haase *et al.*, 2013), Fe--30.5Mn-2.1Al-1.2C (current work), Fe--30Mn-3Al-3Si (Vercammen *et al.*, 2004), and Fe-30.5Mn-8.0Al-1.2C (current work) steels.

The structure features of the 2Al steel as slip and twinning can be observed in Fig. 5 at strain of 0.11 and 0.51 by means of IQ maps, KAM maps, and misorientation angle profile graphs, where low angle grain boundaries can be associated to slip and misorientation angle of 60° is related to twinning. Red lines on the IQ maps are twin boundaries and black lines are high angle grain boundaries. Fig 5 also shows their respective KAM maps. The point-to-origin and point-to-point misorientation profiles are shown on the respective graphs.

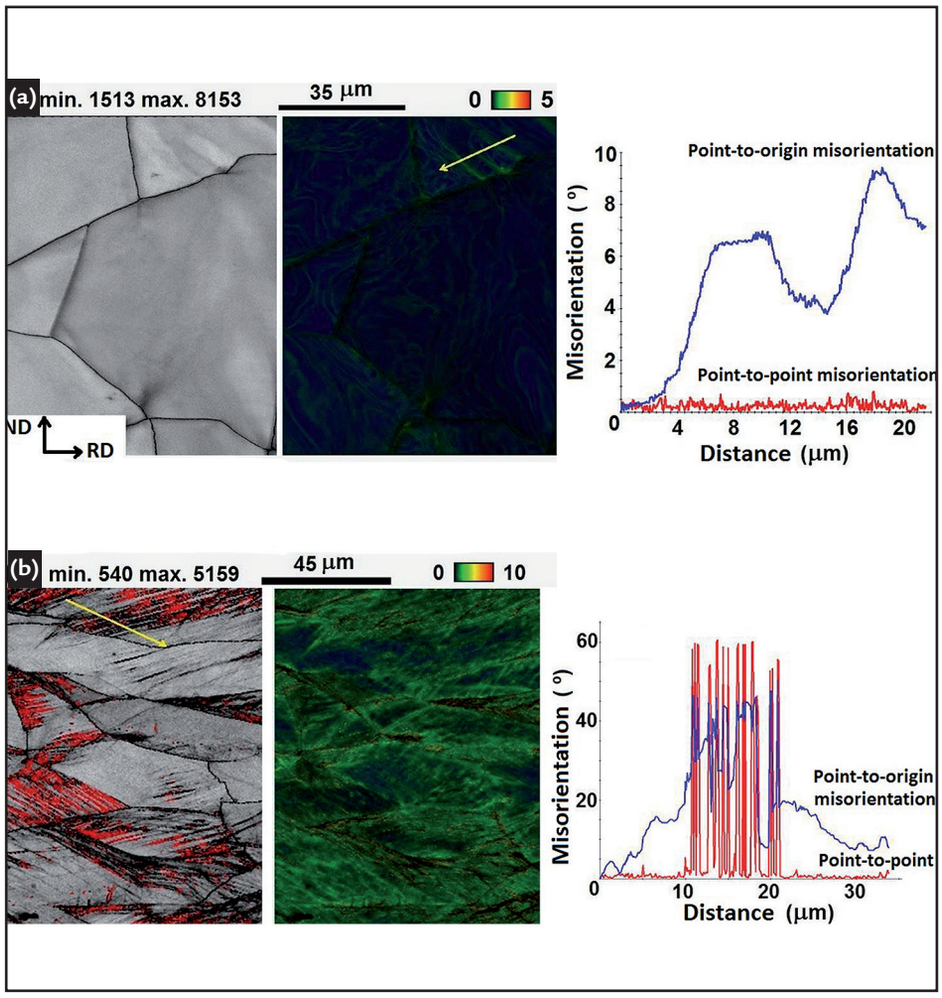


Figure 5
IQ maps, KAM maps, and misorientation profile graphs along the arrows on the maps for the 2Al steel at strains of (a) 0.11 and (b) 0.51. Red lines on the IQ maps are twin boundaries and black lines are high angle grain boundaries. Minimum and maximum values are also indicated in the IQ map gray scale.

## 4. Discussion

Structures with dislocation refinement and deformation twinning (TWIP effect), Fig. 5, are the major contributors for the resultant extreme mechanical properties of the 2Al steel. The misorientation profile graphs show that low angle grain boundaries, as indicated by the point-to-point misorientation, can be associated to slip at low strain and misorientation of 60° is related to twinning at high strain. This implies that 2Al steel has deformed microstructure similar to that of other TWIP steels (Vercammen *et al.*, 2004, Bracke et al., 2012, and Haase et al., 2013, Souza *et al*, 2016).

It is suggested that dislocation sources were activated in order to fulfill slip planes, which became exhausted

of dislocations, owing to deformation stresses, developing slip bands and activating new dislocation sources in the 8Al steel at a low to medium strain (Fig. 2 at strain of 0.22). These dislocations may be seen among crystallographic slip bands in Fig. 2 at strain of 0.22. This conduced a refinement of the slip band substructure at medium strains with good similarity to those seen in another recent work (Welsch *et al*., 2016). Fig. 1b shows SB with twins, mechanical twinning, and remained slip band substructure for the cold rolled 8Al steel at higher strain level (> 0.36). Fig. 1c shows the respective KAM maps from the microstructures of the 8Al steel, where it can be seen that the deformation energy has been accommodated in planar slip or slip bands at low and medium strains, whereas at higher strains the deformation energy is accommodated mainly in shear bands and twins as shown by the high variation on the KAM angle range. The deformation energy is accommodated by slip at low strain level, while at high strain, it is accommodated mainly by profuse mechanical twinning in the 2Al steel (Fig. 5).

Fig. 1 and Fig. 3b show that the intensity of the mechanical twinning at strain of 0.69 for 2Al steel is higher than that of 8Al steel. This means that gradual addition of Al amounts in Fe-Mn-Al-C alloys contributes to the SFE increase (Oh *et al.,* 1995, Park et al., 2010), which reduces twin formation (Li *et al*., 2008)[29]; that is, low-SFE alloys commonly deform by mechanical twins, developing an alloy type texture. Furthermore, for high-SFE metals, deformed by dislocation slip at room temperature, the pure metal type texture is developed as observed in the 8Al steel (Figs. 3a) (Hirsch *et al*., 1988, Leffers et al., 2009, and Souza *et al*., 2012). In order to better represent the texture evolution for both cold rolled steels their ODFs are gathered in Fig. 3.

Fig. 3a shows that the intensity of the Goss-type texture becomes high with increasing deformation, demonstrating the dependence of the heterogeneous microstructure (Fig. 1) with the Goss component formation. This microstructural heterogeneous occurrence can be seen in the two steels (Fig. 1). It has been reported that stacking faults and interactions of perfect dislocations probably controlled the crystallographic twin growth in the 2Al steel by comparing with other alloys (Idrissi *et al*., 2010). Brass-type texture occurrence in the 2Al steel (Fig. 3a) is attributed to this twin formation. It was observed in other steels (Donadille *et al*., 1989 and Saleh *et al*., 2011) that the formation of SB contributed to the formation of Goss and brass components in the 8Al and 2Al steels at a higher strain (Fig. 3a). The Schmid factor for slip diminished to zero on the operative planes conduct to shear banding at higher strain (Donadille *et al*., 1989), generating these relatively inhomogeneous deformation microstructures in both steels.

Fig. 2 shows that deformation twins are formed on {111} slip traces (Souza *et al*., 2016) to storage further plastic deformation at a strain of 0.69 in the 8Al steel. This suggests that, after full refinement of the crystallographic slip band structure, the nucleation of twins, influenced by the Schmid factor favorable for twinning (Hirsch *et al*., 1988 and Yang *et al*., 2006), may occur by the interaction of dislocation sources with the twinning partials on the mature crystallographic slip bands. This behavior can be explained by the plentiful occurrence of remained dislocations among the crystallographic slip bands and among the mechanical twins in the microstructure as can be seen at strain of 0.69 in Fig. 2. This heterogeneous microstructural mode contributed to Cu-type texture occurrence in the 8Al steel (Fig. 3a). Fig. 2 also shows a bundle of twins inside the shear band, which was related to Goss orientation, and remaining dislocations in the deformed microstructure at higher strain. It is known that the addition of Al in the alloy reduces the formation of mechanical twins, owing to the increase on the critical resolved shear stress required for twin formation when SFE is increased (Hong *et al*., 2012). Accordingly, 8Al steel has lower twinning activity when compared to that of the 2Al (Fig. 3b).

Crystallographic texture can be adjusted by putting an alloy through different processing steps, in which cold rolling is one of them, contributing to an optimization of the grain orientation distribution for the stamping process (Souza *et al*., 2012). In Fig. 4, it can be observed that orientation density on the brass and Goss texture decreased, while the copper texture intensity increased with increasing Al content, for different cold rolled high-Mn (with Mn content close to 30 wt%) steels at a strain of 0.69. This means that, the twin formation reduction with increasing Al content contributes to the decrease on brass- and Goss-type texture intensities, whereas Copper-type texture intensity increases in such cold rolled steels (Fig. 4).

## 4. Conclusions

In summary, comparative evaluation of the microstructures and crystallographic textures was done for the cold rolled Fe-30.5Mn-2.1Al-1.2C and Fe-30.5Mn-8.0Al-1.2C (wt%) low-density high-Mn steels, by means of EBSD and ECCI techniques. Slip was observed in both steels at low strain. Deformation twinning and shear banding contributed to the formation of strong Goss- and brass-texture in the 2Al steel at a high strain. It has been suggested that activation of dislocations may develop the crystallographic slip bands and their refinement at a low to medium rolling strain in the 8Al steel. For such steel, it was also suggested that the nucleation of twins, after full refinement of the crystallographic slip band structure, may occur by the interaction of dislocation sources with the twinning partials on the mature slip bands. KAM maps showed that the stored deformation energy was mainly localized in the twinned areas and shear bands, generating the inhomogeneous deformation microstructures in both steels at a higher strain. These microstructural heterogeneities contributed to the Copper- and Goss-texture in the 8Al steel at such strain. Comparative result showed that Goss and Brass texture intensity decreases and Cu-texture increases as the Al wt.% increases in cold rolled High-Mn (with Mn close to 30 wt.%) steels.

## Acknowledgements

The author acknowledge the *CNPq* (Brazil) for postdoctoral fellowship (process number: 237863/2012-0), German Research Foundation in the framework of the SFB 761 – steel ab initio, and also thank Gutierrez-Urrutia I. and Raabe D. for their very much appreciated inputs.

## References


BOUAZIZ, O., ALLAIN, S., SCOTT, C.P., CUGY, P., BARBIER, D. High manganese austenitic twinning induced plasticity steels: A review of the microstructure properties relationships. ***Current Opinion in Solid State and Materials Science,*** v. 15, p. 141-168, 2011.

BRACKE, L., VERBEKEN, K., KESTENS, L. Texture generation and implications in TWIP steels. ***Scripta Materialia,*** v. 57, p. 1007-1011, 2012.

DE COOMAN, B. C., CHIN, K.-G., KIM, J. High Mn TWIP Steels for automotive applications. ***New Trends and Developments in Automotive System Engineering,*** p. 101-128, 2011.

DONADILLE, C., VALLE, R., DERVIN, P., PENELLE, R. Development of texture and microstructure during cold-rolling and annealing of f.c.c. alloys: example of an austenitic stainless steel. ***Acta Metallurgica et Materialia,*** v. 37, p. 1547-1571, 1989.

GUTIERREZ-URRUTIA, I., RAABE, D. Multistage strain hardening through dislocation substructure and twinning in a high strength and ductile weight-reduced Fe–Mn–Al–C steel. ***Acta Materialia,*** v. 60, p. 5791–5802, 2012.

GUTIERREZ-URRUTIA, I., RAABE, D. High strength and ductile low density austenitic FeMnAlC steels: simplex and alloys strengthened by nanoscale ordered carbides. ***Materials Science and Technology,*** v. 30, p. 1099-1104, 2014.

HAASE, C., CHOWDHURY, S. G., BARRALES-MORA, L. A., MOLODOV, D. A., GOTTSTEIN, G. On the relation of microstructure and texture evolution in an austenitic Fe-28Mn-0.28C TWIP steel during cold rolling. ***Metalurgical and Materials Transactions A,*** v. 44A, p. 911-922, 2013.

HIRSCH, J., LÜCKE, K., HATHERLY, M. Overview n. 76: mechanism of deformation and development of rolling textures in polycrystalline f.c.c. Metals-III. The influence of slip inhomogeneities and twinning. ***Acta Metallurgica,*** v. 36, p. 2905-2927, 1988.

HONG, S., SHIN, S. Y., KIM, H. S., LEE, S., KIM, S.-K., CHIN, K.-G., KIM, N. J. Effects of aluminum addition on tensile and cup forming properties of three twinning induced plasticity steels. ***Metallurgical and Materials Transactions A,*** v. 43, p. 1870-1883, 2012.

IDRISSI, H., RENARD, K., RYELANDT, L., SCHRYVERS, D., JACQUES, P. J. On the mechanism of twin formation in Fe-Mn-C TWIP steels. ***Acta Materialia,*** v. 58, p. 2464-2476, 2010.

LEFFERS, T., RAY, R. K. The brass-type texture and its deviation from the copper-type texture. ***Progress in Materials Science,*** v. 54, p. 351-396, 2009.

LI, H., YIN, F., SAWAGUCHI, T., OGAWA, K., ZHAO, X., TSUZAKI, K. Texture evolution analysis of warm-rolled Fe-28Mn-6Si-5Cr shape memory alloy. ***Materials Science and Engineering A,*** v. 494, p. 217-226, 2008.

OH, B.W., CHO, S.J., KIM, Y.G., KIM, Y.P., KIM, W.S., HONG, S.H. Effect of aluminium on deformation mode and mechanical properties of austenitic Fe-Mn-Cr-Al-C alloys. ***Materials Science and Engineering A,*** v. 197, p. 147-156, 1995.

PARK, K.-T., JIN, K. G., HAN, S. H., HWANG, S. W., CHOI, K., LEE, C. S. Stacking fault energy and plastic deformation of fully austenitic high manganese steels: effect of Al addition. ***Materials Science and Engineering A,*** v. 527, p. 3651-3661, 2010.

RAY, R. K. Rolling textures of pure nickel, nickel-iron and nickel-cobalt alloys. ***Acta Metallurgica et Materialia,*** v. 43, p. 3861-3872, 1995.

SALEH, A. A., PERELOMA, E. V., GAZDER A. A. Texture evolution of cold rolled and annealed Fe–24Mn–3Al–2Si–1Ni–0.06C TWIP steel. ***Materials Science and Engineering A,*** v. 528, p. 4537-4549, 2011.

SOUZA, F. M., PADILHA, A. F., GUTIERREZ-URRUTIA, I., RAABE, D. Microstructural analysis in the Fe-30.5Mn-8.0Al-1.2C and Fe-30.5Mn-2.1Al-1.2C steels upon cold rolling. ***REM – International Engineering Journal,*** v. 69, n.2, p. 167-173, 2016.

SOUZA, F. M., PADILHA, A. F., GUTIERREZ-URRUTIA, I., RAABE, D. Texture evolution in the Fe-30.5Mn-8.0Al-1.2C and Fe-30.5Mn-2.1Al-1.2C steels upon cold rolling. ***REM – International Engineering Journal,*** v. 69, n.1, p. 59-65, 2016.

SOUZA, F. M., PLAUT, R. L., LIMA, N. B., FERNANDES, R. C., PADILHA, A. F. Recrystallization and crystallographic texture in AA4006 aluminum alloy sheets produced by twin roll caster and direct chill processes. ***REM – International Engineering Journal,*** v. 65, n.3, p. 363-370, 2012.

SPRINGER, H., RAABE, D. Rapid alloy prototyping: compositional and thermo-mecha-

nical high throughput bulk combinatorial design of structural materials based on the example of 30Mn-1.2C-xAl triplex steels. ***Acta Materialia,*** v. 60, p. 4950–4959, 2012.

VERCAMMEN, S., BLANPAIN, B., DE COOMAN, B.C., WOLLANTS, P. Cold rolling behaviour of an austenitic Fe–30Mn–3Al–3Si TWIP-steel: the importance of deformation twinning. ***Acta Materialia,*** v. 52, p. 2005–2012, 2004.

WELSCH, E., PONGE, D., HAFEZ HAGHIGHAT, S.M., SANDLOBES, S., CHOI, P., HERBIG, M., ZAEFFERER, S., RAABE, D. Strain hardening by dynamic slip band refinement in a high-Mn lightweight steel. ***Acta Materialia,*** v. 116, p. 188-199, 2016.

YANG, P., XIE, Q., MENG, L., DING, H., TANG, Z. Dependence of deformation twinning on grain orientation in a high manganese steel. ***Scripta Materialia,*** v. 55, p. 629-631, 2006.

Received: 23 January 2017 - Accepted: 20 March 2017.